

Transition by Intermittency in Granular Matter: From Discontinuous Avalanches to Continuous Flow

Raphaël Fischer, Philippe Gondret, and Marc Rabaud

Lab FAST, CNRS, Université Paris-Sud, Université Pierre et Marie Curie-Paris 6, Bâtiment 502, Campus universitaire, F-91405 Orsay cedex, France

(Received 5 June 2009; published 17 September 2009)

We investigate, in the rotating drum configuration, the transition from the regime of discontinuous avalanches observed at low angular velocity to the regime of continuous flow observed at higher velocity. Instead of the hysteretic transition reported previously by Rajchenbach [Phys. Rev. Lett. **65**, 2221 (1990)], with an apparent bistability of the two flow regimes in a range of drum velocities, we observe intermittency with spontaneous erratic switches from one regime to the other. Both scenarios of transition are recovered by a model dynamic equation for the avalanche flow with two sources of stochasticity: a Langevin noise during the avalanche flow and a distributed maximal stability angle at which avalanches start.

DOI: 10.1103/PhysRevLett.103.128002

PACS numbers: 45.70.Ht, 05.45.-a

Transitions from discontinuous to continuous dynamics under the action of a continuous driving force are observed in a large number of systems: solid friction [1], fracture propagation [2], peeling [3], granular avalanches [4], outgassing in a non-Newtonian fluid [5], Josephson junction [6], etc. We report here an original transition by temporal intermittency in the framework of granular flow. In recent years great effort has been made to understand the complex rheology of dense granular flows [7]. One usual flow geometry is a horizontal rotating drum partially filled with grains. The interest of this device lies in the experimental simplicity of its closed geometry, and also in its use in many industries such as civil engineering or pharmaceuticals involving mixing or segregation of gravels, sand or powders [8]. Depending on the angular velocity Ω of the rotating drum, different regimes are classically observed when increasing Ω : discrete avalanching, continuous flow with flat interface, S-shape interface, and finally centrifugation. In the following we will concentrate on the first transition from *discrete avalanches* (DA) to *continuous flow* (CF) that arises typically when $\Omega \sim \Delta\theta/\tau$, where $\Delta\theta = \theta_m - \theta_r$ is the typical avalanche amplitude and τ the typical avalanche duration, i.e., the time for the slope of the pile to relax from the angle of maximal stability θ_m towards the angle of repose θ_r [4]. This transition has been reported to be hysteretic by Rajchenbach [9] in a short cylinder: He observed that in a range of Ω values, the regime can be either DA or CF depending on the flow history. In a long cylinder, Caponeri *et al.* [4] reported both a smaller hysteresis and a spatial coexistence of DA and CF domains in the transition zone. In a different flow configuration where a granular heap is fed from the top, Lemieux *et al.* [10] report a sharp DA-CF transition without any hysteresis. The argument invoked for the hysteretic behavior was either a difference of typical grain falling time in the DA and CF regime [9], a difference between the static

and dynamic effective friction coefficients [4], or stochastic fluctuations in the grain flow [11]. In this Letter, we present rotating drum experiments exhibiting in a given rotation velocity range a progressive flow transition by temporal intermittency instead of a hysteresis scenario: The two flow regimes are found both unstable rather than both stable in this Ω range. We explain the observed spontaneous and erratic switches from one regime to the other by the intrinsic dissipation and fluctuation of granular flows.

The experimental setup is a rotating cylinder of diameter $2R = 20$ cm and width $b = 5$ cm half-filled with glass beads of diameter $d = 0.95 \pm 0.05$ mm. A microstep motor followed by a huge reduction factor imposes a smooth continuous rotation with an excellent resolution [12]. With a video camera (750×500 pixels, 50 images/s), the entire pile is recorded and the pile surface is detected by image processing. The flow is localized in a thin surface layer and the interface remains flat at all time t [13], so that we measure its instantaneous slope angle $\theta(t)$ with a typical resolution of 0.01° over long experimental runs (roughly half of an hour for each) where the drum rotation is kept constant.

At low drum velocity Ω (< 0.7 deg/s), only the DA regime is observed with a typical avalanche amplitude $\Delta\theta = 1.7 \pm 0.3^\circ$ and typical avalanche duration $\tau = 0.9 \pm 0.1$ s. Note that we do not measure any significant variation of $\Delta\theta$ or τ with Ω . At high enough Ω (> 1.2 deg/s), only the CF regime is observed, with a flat interface of constant slope angle. In between, no hysteresis but temporal intermittency between the DA and CF regimes is observed as shown in Fig. 1(a), where the DA regime appears in red (light gray) whereas the CF regime appears in blue (dark gray). In the DA regime, the slope angle θ ranges from the angle of repose $\theta_r = 23.2 \pm 0.1^\circ$ to the angle of maximal stability $\theta_m = 24.9 \pm 0.2^\circ$,

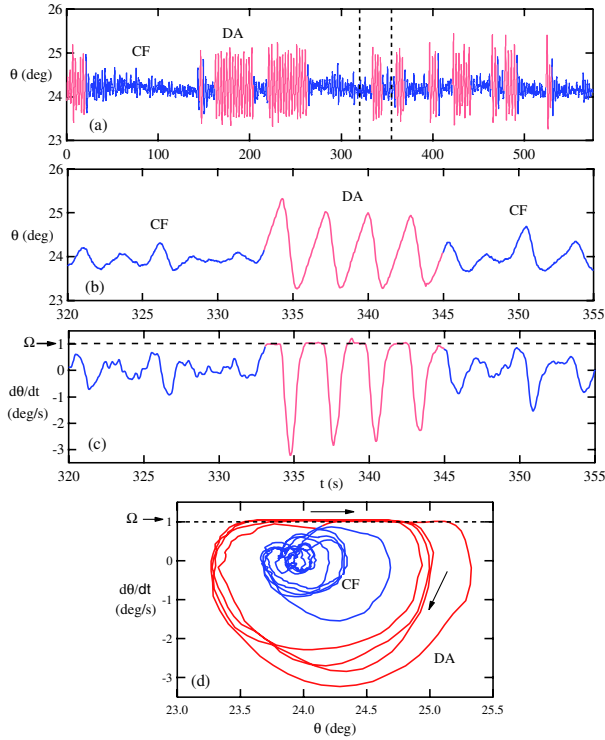


FIG. 1 (color online). (a) Time evolution of the mean slope angle θ of the pile for $\Omega = 1.02$ deg/s. (b) Zoom of $\theta(t)$ on the time window delimited by the two vertical dotted lines in (a). (c) Time derivative of the slope angle $\dot{\theta}$ in the zoomed time window and (d) corresponding phase portrait $(\theta, \dot{\theta})$. The DA regime is plotted in red (light gray) and the CF regime in blue (dark gray).

whereas in the CF regime, the angle fluctuations are one order of magnitude smaller ($\theta = 24.2 \pm 0.1^\circ$). Detailed switches between DA and CF regimes are put in evidence in a zoom on Fig. 1(a) presented in Fig. 1(b). Figure 1(c) shows the corresponding $\dot{\theta}(t)$ plot, and Fig. 1(d) the phase portrait $(\theta, \dot{\theta})$. The time derivative $\dot{\theta}$ is related to the avalanche grain flux q at the drum center by $q = (bR^2/2)(\Omega - \dot{\theta})$ from mass conservation [4,14]. The time periods when the pile is at rest with respect to the drum (solid rotation without any grain flow) can be easily determined from Fig. 1(c) as $\dot{\theta} = \Omega$, and the time the system spends in the DA regime can thus be determined precisely. In the CF regime, $\dot{\theta}$ fluctuates around zero, but does not reach the Ω value. In the phase portrait $(\theta, \dot{\theta})$ of Fig. 1(d), the DA regime appears as large clockwise loops that are flattened on the top. The flat parts correspond to the pile at rest whose angle θ increases at the rate Ω , and the curved parts correspond to the θ relaxation during avalanches with downward grain flux q ($\dot{\theta} < \Omega$). In the CF regime, the system fluctuates around the fixed point ($\theta = 24.2^\circ$, $\dot{\theta} = 0$). Transition from CF to DA occurs when $\dot{\theta}$ reaches Ω because of a sufficiently large fluctuation in the grain flux: The pile comes to rest and its angle θ starts increasing linearly with time at the rate $\dot{\theta} = \Omega$ until the next ava-

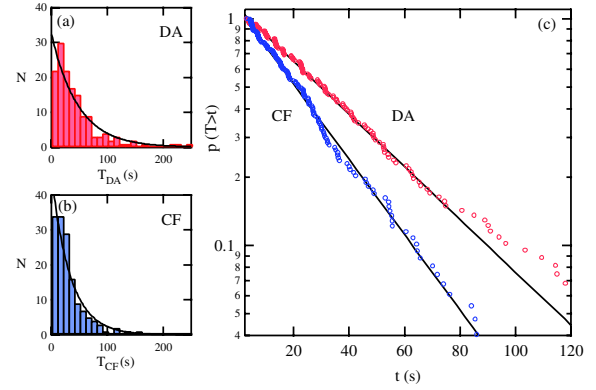


FIG. 2 (color online). Distribution of life time T of (a) DA and (b) CF regime for $\Omega = 0.99$ deg/s. (c) Corresponding survival function $p(T > t)$. The solid lines correspond to exponential fits $\exp(-T/\bar{T})$ with (a) $\bar{T}_{DA} = 48$ s and (b) $\bar{T}_{CF} = 33$ s.

lanche starts. Conversely, transition from DA to CF occurs when an avalanche starts at a low enough angle θ_m so that the trajectory fails reaching the line $\theta = \Omega$ but gets trapped by the fixed point.

The distributions of life times of both regimes are shown in Fig. 2: For both DA and CF regimes, small life time events are more frequent than large ones. Indeed the distributions of life time T follow a decreasing exponential law $N \sim \exp(-T/\bar{T})$ with a characteristic mean life time \bar{T} , as evidenced by the linear decrease of the complementary cumulative density function (survival function) in the log-lin plot of Fig. 2(c).

Let us now report on what happens when the drum velocity is varied. The evolution of the mean life time \bar{T} of each regime is shown in Fig. 3 as a function of the drum rotation velocity Ω : The mean life time of the CF regime increases roughly exponentially with Ω , whereas the mean life time of the DA regime decreases the same way. We indeed observe experimentally small bursts of CF regime interrupting long DA periods at lower drum velocity ($\Omega \approx 0.8$ deg/s) and the contrary at higher drum velocity

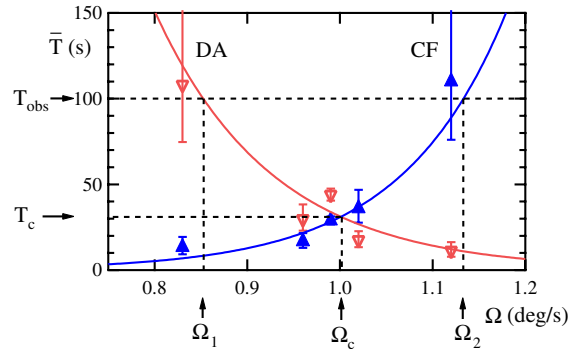


FIG. 3 (color online). Mean life time \bar{T} of DA regime (∇) and CF regime (\blacktriangle) as a function of Ω . (---) Exponential fits $\bar{T} = T_c \exp[\beta(\Omega - \Omega_c)/\Omega_c]$ with $T_c = 30$ s, $\Omega_c = 1$ deg/s, $\beta_{DA} = -7.9$ and $\beta_{CF} = 8.9$.

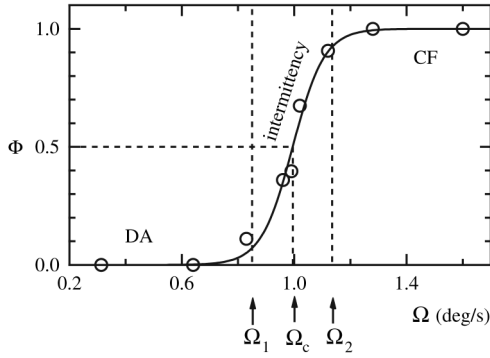


FIG. 4. Mean time fraction ϕ of the CF regime as a function of the drum rotation velocity Ω . Experimental data points (\circ) and fit by a tanh curve (-).

($\Omega \approx 1.1$ deg/s). The scenario of this progressive DA-CF transition by intermittency can be simply viewed when plotting the time fraction ϕ the system spends in the CF regime over a long observation time as a function of the drum rotation velocity Ω (Fig. 4): ϕ increases gradually from 0 at low Ω towards 1 at high Ω . The middle of the transition occurs at $\Omega_c \approx 1$ deg/s with an equal mean duration of each regime $T_c \approx 30$ s (Fig. 3). As $\phi(\Omega) = \bar{T}_{CF}/(\bar{T}_{DA} + \bar{T}_{CF})$ data of Fig. 4 can be fitted by a tanh function. Obviously, ϕ is independent of the starting regime, but its precise measurement requires an observation time T_{obs} greater than the highest of the two life times. For, e.g., $T_{obs} \approx 100$ s, Fig. 3 shows that intermittency between the two regimes will only be observed in the range from $\Omega_1 \approx 0.85$ deg/s to $\Omega_2 \approx 1.13$ deg/s. For $\Omega < \Omega_1$, $\bar{T}_{DA} > T_{obs}$ and the DA regime only will be observed and will appear as stable. Reciprocally, the CF regime only will be observed and appear as stable when $\Omega > \Omega_2$ ($\bar{T}_{CF} > T_{obs}$). For small observation time ($T_{obs} < T_c$), Ω_1 is greater than Ω_2 and both regimes will appear as stable in the $\Omega_2 < \Omega < \Omega_1$ range: The transition will then appear as hysteretic.

Let us now present a simple model reproducing the observed complex dynamics. Considering the velocity profile measurements of [13] for the thin surface flowing layer, we reduced the avalanche flow dynamics in the case of negligible drum rotation to a model equation for the pile angle θ and its time derivatives describing the slope relaxation dynamics in [14]. The velocity v of the flowing layer being proportional to slope relaxation $\dot{\theta}$ and introducing a velocity dependent dynamic friction coefficient $\mu(v) = \mu_n + \gamma v^2$, the resulting dynamic equation was:

$$\ddot{\theta} + A(\theta - \theta_n) = B\dot{\theta}^2. \quad (1)$$

In this equation, the first term corresponds to the grain acceleration, and the second term corresponds to the action of gravity force minus the dynamical friction force at vanishing grain velocity ($\tan\theta_n = \mu_n$). Finally, the right-hand side term describes the quadratic increase of friction

force with grain velocity. An avalanche starting from rest at an angle θ_m above the “neutral” angle θ_n develops and stops at a lower angle $\theta_r < \theta_n$. By contrast, no avalanche can develop starting below θ_n . Parameters A and B both depend on the drum geometry and on the grain properties. Parameter A scales as $1/\tau^2$ where τ is the mean avalanche duration. Parameter B characterizes the granular dissipation: the larger B , the larger the dissipation and the $\theta(t)$ curve asymmetry with respect to the neutral angle θ_n : $\theta_n - \theta_r < \theta_m - \theta_n$. By extensive experiments, we validated this differential equation involving small angle variations around the neutral angle θ_n and measured its coefficients [14]. Following Ref. [11], we now extend this deterministic equation for the granular flow to non-negligible drum rotation velocity Ω :

$$\ddot{\theta} + A(\theta - \theta_n) = B(\dot{\theta} - \Omega)^2 + \epsilon(t). \quad (2)$$

The addition of a small random Langevin-type force term $\epsilon(t)$ is consistent with the Gaussian fluctuations we measured experimentally for $\ddot{\theta}$ in the flowing phases. In this equation for the global variable θ , this stochastic term stands for fluctuations of collisional forces at the grain level. Equation (2) describes avalanche flows (i.e., when $\dot{\theta} < \Omega$) and must be completed by the condition of whole solid rotation $\dot{\theta} = \Omega$ during the rest phase and by a random starting angle reproducing the experimental distribution of

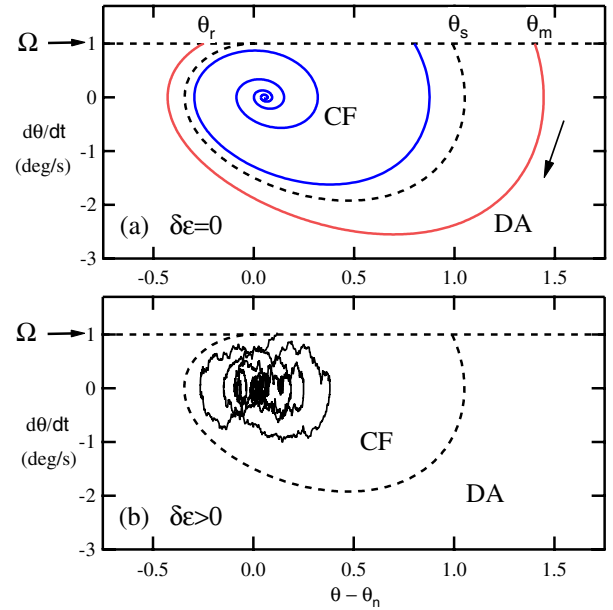


FIG. 5 (color online). Numerical phase portrait $(\theta - \theta_n, \dot{\theta})$ from Eq. (2) for $\Omega = 1$ deg/s ($A = 8$ s $^{-2}$, $B = 0.45$ deg $^{-1}$). (a) Calculated trajectory for $\delta\epsilon = 0$ starting from the initial values (1.4,1) or (0.8,1). (b) Calculated CF trajectory for $\delta\epsilon = 8$ deg/s $^{-2}$ starting from the fixed point. The horizontal dashed line corresponds to $\dot{\theta} = \Omega$ and the curved dashed line corresponds to the separatrix between the DA and CF regimes starting from (θ_s, Ω) and that reaches a maximum value of $\dot{\theta}$ when $\dot{\theta} = \Omega$.

θ_m [14]. Figure 5(a) shows two different avalanche trajectories calculated from Eq. (2) with zero noise and starting from an initial pile at rest in the DA regime. The curve asymmetry ($\theta_n - \theta_r < \theta_m - \theta_n$) is a consequence of dissipation ($B \neq 0$). As a consequence, two different behaviors are observed depending on the starting angle: For $\theta_m > \theta_s$, the outer avalanche trajectory in red (light gray) stops at θ_r when $\dot{\theta} = \Omega$. For $\theta_m < \theta_s$, the inner avalanche trajectory in blue (dark gray) spirals towards the CF fixed point. The dashed curve starting from θ_s is the separatrix between these two behaviors corresponding to the DA and CF regimes. Note that this curve and in particular θ_s depend on the Ω value. In this escape scenario from the DA regime to the CF regime, the probability is mainly ascribed to the probability to sort a θ_m angle smaller than $\theta_s(\Omega)$, a probability that increases strongly with Ω since θ_s increases with Ω . Note that this transition does not require a particular noise level ϵ . This is confirmed experimentally as we indeed observe that the DA \rightarrow CF transitions occur for the lowest values of the starting angle distribution. This indicates that the characteristic value Ω_1 above which this transition can be observed for a given observation time T_{obs} ($T_{\text{DA}} \leq T_{\text{obs}}$) is not very sensitive to the noise level (Ω_1 should only slightly decrease for increasing noise level ϵ).

Figure 5(b) results from the simulation of Eq. (2) for a nonzero noise level and starting from the fixed point in the CF regime. The system remains in the CF regime as long as $\dot{\theta}$ does not reach the solid rotation value Ω . By contrast to the previous case, the time of escape from the CF regime only depends on the noise level ϵ : The fixed point of the CF regime is found linearly stable at any Ω and can only be destabilized by a non zero noise level. At first order, the $\dot{\theta}$ (grain flux) fluctuation denoted $\delta\dot{\theta}$ increases linearly with the noise standard deviation $\delta\epsilon = \langle \epsilon^2 \rangle^{1/2}$ and the CF \rightarrow DA transition is likely as soon as $\delta\dot{\theta} \sim \Omega$ [Fig. 5(b)]. As a consequence, the corresponding characteristic transition value Ω_2 increases linearly with increasing noise.

A sketch of Ω_1 and Ω_2 variations with the noise level $\delta\epsilon$ is presented in Fig. 6 for a given T_{obs} : For large $\delta\epsilon$, $\Omega_2 > \Omega_1$, so that in the range $\Omega_1 < \Omega < \Omega_2$ both DA and CF regime are observed. The flow regime presents intermittency and switches randomly from one solution to the other as observed in the present experiment. In the peculiar case of low enough noise level ϵ , $\Omega_2 < \Omega_1$ so that both regimes appear as stable in the range $\Omega_2 < \Omega < \Omega_1$: Since both DA and CF life times are larger than the observation time T_{obs} , either DA or CF regime can be observed depending on the flow history of the system, which makes the transition apparently hysteretic as described by Rajchenbach [9].

To conclude, we observe a progressive transition by intermittency between the regime of discrete avalanches and the regime of continuous granular flow in a rotating drum when varying the rotation velocity Ω of the drum.

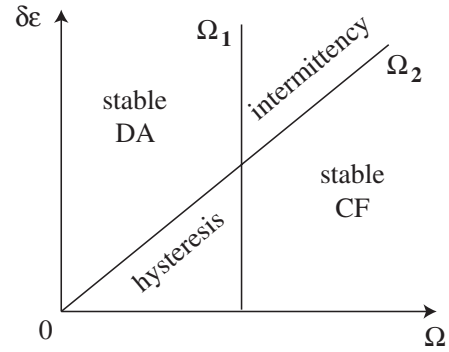


FIG. 6. Sketch of the state diagram given by model Eq. (2) with critical velocities Ω_1 and Ω_2 as functions of the noise level $\delta\epsilon$ for a given observation time T_{obs} .

This transition occurs gradually in a range of Ω by the appearance of increasing bursts of one regime in the other, in contrast to the hysteretic transition reported by [9]. Both scenarios of transition can be explained by a flow modeling with dissipation, depending on the fluctuation level and on the observation time. We also suggest that the spatiotemporal intermittency reported by [4] in a spatially extended system (long rotating drum) can be understood in this frame. The role of fluctuations appears crucial in the intermittency that is also observed in solid friction, fracture, or even in time reversal of the magnetic field [1,2,15].

We acknowledge C. Delacour and Y. Texier for their help in the measurements, and B. Perrin, P. Manneville, V. Hakim and E. Trizac for warm and fruitful discussions.

-
- [1] T. Baumberger, F. Heslot, and B. Perrin, *Nature (London)* **367**, 544 (1994).
 - [2] R. Blumenfeld, *Phys. Rev. Lett.* **76**, 3703 (1996).
 - [3] M. Barquins and M. Ciccotti, *Int. J. Adhes. Adhes.* **17**, 65 (1997).
 - [4] M. Caponeri *et al.*, in *Mobile Particulate Systems*, edited by E. Guazzelli and L. Oger (Kluwer Academic Publishers, Dordrecht, 1995), pp. 331–336.
 - [5] T. Divoux *et al.*, *Phys. Rev. E* **79**, 056204 (2009).
 - [6] E. Ben-Jacob *et al.*, *Phys. Rev. Lett.* **49**, 1599 (1982).
 - [7] GDR MiDi, *Eur. Phys. J. E* **14**, 341 (2004).
 - [8] J.M. Ottino and D.V. Khakkar, *Annu. Rev. Fluid Mech.* **32**, 55 (2000).
 - [9] J. Rajchenbach, *Phys. Rev. Lett.* **65**, 2221 (1990).
 - [10] P.-A. Lemieux and D. J. Durian, *Phys. Rev. Lett.* **85**, 4273 (2000).
 - [11] S. J. Linz, W. Hager, and P. Hänggi, *Chaos* **9**, 649 (1999).
 - [12] S. Courrech du Pont *et al.*, *Phys. Rev. Lett.* **90**, 044301 (2003); *Europhys. Lett.* **61**, 492 (2003).
 - [13] S. Courrech du Pont *et al.*, *Phys. Rev. Lett.* **94**, 048003 (2005).
 - [14] R. Fischer *et al.*, *Phys. Rev. E* **78**, 021302 (2008).
 - [15] F. Ravelet *et al.*, *Phys. Rev. Lett.* **101**, 074502 (2008).